Ticks and Tick-borne Diseases 10 (2019) 1135–1141

Contents lists available at ScienceDirect

Ticks and Tick-borne Diseases

journal homepage: www.elsevier.com/locate/ttbdis

Crystal structure of *Borrelia burgdorferi* outer surface protein BBA69 in comparison to the paralogous protein CspA

Kalvis Brangulis[a,*], Inara Akopjana[a], Ivars Petrovskis[a], Andris Kazaks[a], Kaspars Tars[a,b]

[a] Latvian Biomedical Research and Study Centre, Ratsupites 1 k-1, LV-1067, Riga, Latvia
[b] University of Latvia, Faculty of Biology, Jelgavas 1, LV-1004, Riga, Latvia

ARTICLE INFO

Keywords:
Ixodes ticks
Spirochetes
Paralogous proteins
X-ray crystallography

ABSTRACT

The spirochete *Borrelia burgdorferi* sensu lato is the causative agent of Lyme borreliosis – the most common tick-borne disease in Europe and the United States. Spirochetes are transmitted from infected *Ixodes* ticks to the mammalian host when the ticks feed. In general, the transfer process of the borreliae is quite complicated, as the environments in the tick and the new mammalian host differs significantly. Therefore, *Borrelia* changes the expression profile of dozens of proteins, mainly outer surface proteins, to adapt to the new tasks and needs in the new organism. In the transfer process from the tick to the mammalian host, spirochetes that cause Lyme disease show the strongest upregulation of members of paralogous gene family 54 (PFam54). PFam54 members encode 10 proteins, and BBA69 is one of its members. Although several PFam54 members play an important role in the pathogenesis of Lyme disease, the exact function has been determined only for CspA, which binds complement regulator factor H (CFH) and factor H-like protein 1 (FHL-1); thus, CspA is essential to resist the vertebrate host's immune response. In the current study, we determined the crystal structure of BBA69 at a 2.25 Å resolution. The BBA69 structure revealed a seven α-helical BbCRASP-1 fold previously found only in PFam54 member proteins. Among the PFam54 members, BBA69 shares the highest sequence identity (61%) and 3-D similarity with CspA. Although none of the PFam54 members besides CspA bind CFH and FHL-1, in the current study, we investigated the structural differences accounting for the divergence in the functions of these proteins. The results clearly indicated that the C-terminal α-helix is the main determinant of this functional divergence. The results provide better insight into the PFam54 proteins that play an important role in the pathogenesis of Lyme disease.

1. Introduction

Lyme disease, also known as Lyme borreliosis, is a vector-borne infectious disease caused by the spirochete *Borrelia burgdorferi* sensu lato complex bacteria that includes several species such as *B. burgdorferi* sensu stricto (hereafter *B. burgdorferi*), *B. afzelii*, *B. garinii*, *B. spielmanii* and *B. bavariensis* (Burgdorfer et al., 1982; Margos et al., 2013; Rudenko et al., 2011; Steere et al., 2004). For the causative agent of Lyme disease to infect the mammalian host, the spirochete must find its way from the tick's gut to the new host as an infected *Ixodes* tick starts a blood meal (Radolf et al., 2012). The new environment sets many new tasks and challenges for the spirochete, as after it is transferred to the mammalian host, it must resist the immune response, attach to new targets, bind and utilize nutrients that were unavailable in the tick's gut, spread and proliferate (Steere et al., 2016). To adapt to the new conditions when it is transferred from ticks to mammals or vice versa, *Borrelia* changes its proteome (Brooks et al., 2003; Ojaimi et al., 2003; Tokarz et al., 2004). Under the conditions when spirochetes are ready to enter the mammalian host as the tick starts its blood meal, the most highly upregulated proteins in *B. burgdorferi* are those that belong to paralogous gene family 54 (PFam54) (Angel et al., 2010; Ojaimi et al., 2003; Tokarz et al., 2004). In the current study examined BBA69 together with BBA64, BBA65, BBA66, CspA (BBA68), BBA73, BBI36, BBI38, BBI39 and BBJ41 are the PFam54 family members (Casjens et al., 2000). The genes that code for BBA64, BBA65, BBA66, CspA, BBA69 and BBA73 are located on linear plasmid 54 (lp54) and have attracted special attention because of their upregulation and importance in the pathogenesis of Lyme disease (Casjens et al., 2000). PFam54 member BBA64 is essential to ensure the transfer of spirochetes from the tick's salivary glands to the mammalian host (Gilmore et al., 2010). CspA is a complement regulator factor H (CFH) and factor H-like protein 1 (CFHL-1) and thus acts against the mammalian immune response (Kraiczy et al., 2004a). Although CspA is not the only *B. burgdorferi* protein able to bind CFH and/or CFHL-1, it was essential to protect against the immune

* Corresponding author.
E-mail address: kalvis@biomed.lu.lv (K. Brangulis).

https://doi.org/10.1016/j.ttbdis.2019.06.009
Received 19 March 2019; Received in revised form 13 May 2019; Accepted 10 June 2019
Available online 11 June 2019
1877-959X/

response in mice (Hart et al., 2018; Kraiczy and Stevenson, 2013). Additionally, it was demonstrated that BBA66 and BBA73 are necessary to ensure the successful colonization of the spirochete in the mammalian host (Gilmore et al., 2008; Patton et al., 2013). In general, all the previous studies mentioned clearly indicated that the functions of PFam54 members are different. In some respect, their functional diversification is also indicated by the fact that PFam54 members display rather low mutual sequence identities, although their overall fold is well conserved (Brangulis et al., 2013a, 2014; Brangulis et al., 2013b; Cordes et al., 2006b). The PFam54 members CspA and BBA69 show the highest sequence identity among all the PFam54 members at 61%. In comparison, CspA and BBA64 share only 17% sequence identity, but CspA and BBA73 share 14% sequence identity. Despite the comparatively high sequence identity between CspA and BBA69, BBA69 lacks the ability to bind CFH or CFHL-1 and the exact function of BBA69 is still unknown (Kraiczy et al., 2006). The CspA protein has been the subject of thorough structure-function studies and compared with BBA69 to understand the basis for their different functions and the important residues involved in CFH and CFHL-1 binding (Kraiczy et al., 2006, 2009; Wywial et al., 2009). In the current study, we solved the crystal structure of BBA69 to examine the structural differences between the two proteins in molecular detail and to understand the reasons for the functional differences between both proteins. Additionally, the results provide the opportunity to better understand PFam54 proteins, which play potentially important roles in the pathogenesis of Lyme disease.

2. Materials and methods

2.1. Cloning and expression of BBA69 and CspA

BBA69 and CspA were PCR-amplified from *B. burgdorferi* B31 genomic DNA and inserted into the pETm-11 expression vector, which contains an N-terminal 6 × His tag followed by a TEV protease cleavage site (the oligonucleotides used for PCR amplification are given in Table 1). In this way, we prepared two different constructs for BBA69 and a construct for CspA that exclude the signal sequence, as judged with SignalP 4.1 and LipoP 1.0 software (Juncker et al., 2003; Petersen et al., 2011), and the unstructured N-terminal region, as judged from comparison with the crystal structures of other PFam54 members (Brangulis et al., 2013a, 2014; Brangulis et al., 2013b; Cordes et al., 2005). Constructs containing the coding regions of $BBA69_{35\text{-}263}$, $BBA69_{76–263}$, $BBA69_{76–263}$ Leu214Met and $CspA_{65\text{-}251}$ were transformed into *Escherichia coli* XL1-Blue cells and grown overnight at 37 °C on LB agar plates containing kanamycin. Separate colonies were picked and transferred into LB medium supplemented with kanamycin. After 24 h, the plasmid DNA was isolated and verified by DNA sequencing before it was transformed into *E. coli* BL21 (DE3) cells and cultivated in 2 × TY media supplemented with kanamycin (10 mg/ml) at 23 °C until reaching an OD_{600} of 0.8-1.0. To induce protein expression, 0.2 mM IPTG was added, and the cells were incubated for an additional 12–14 h. The cells were then harvested by centrifugation at 5000 × g. Se-Met-labeled $BBA69_{76–263}$ Leu214Met was produced with the methods described previously to produce BB0689 protein (Brangulis et al., 2015).

2.2. Purification of BBA69 and CspA

BBA69 was purified by affinity chromatography on a Ni-NTA agarose (Protino) column. Afterwards, the 6 × His tag was removed from the recombinant protein by TEV (*tobacco etch virus*) protease digestion overnight at room temperature. The cleaved 6 × His tag and TEV protease were removed by an additional round of affinity chromatography (Fig. S1). The protein was buffer-exchanged into 10 mM Tris HCl (pH 8.0) and concentrated using an Amicon centrifugal filter unit (Millipore) to a concentration of 11 mg/ml. CspA used in gel filtration chromatography experiment was purified in the same manner as BBA69.

2.3. Estimation of multimeric state by gel filtration chromatography

$BBA69_{76–263}$ (11 mg/ml) in 10 mM Tris HCl (pH 8.0) containing either 0.25 M or 0.5 M NaCl was loaded on a prepacked Superdex 200 10/300 G L column (Amersham Biosciences). Bovine serum albumin (67 kDa), ovalbumin (43 kDa) and chymotrypsinogen A (25 kDa) were used as MW reference standards. To further characterize multimeric state of the protein, $BBA69_{76–263}$ (1 mg/ml) either alone or in mixture with $CspA_{65\text{-}251}$ (1 mg/ml) were loaded on a prepacked Superdex 75 10/300 G L column (Amersham Biosciences) in 10 mM Tris HCl, 200 mM NaCl (pH 8.0) with the flow rate of 0.5 ml/min (Fig. 1). While MW of CspA (22.5 kDa) is close to BBA69 (22.4 kDa), dimerization of CspA is well demonstrated (Cordes et al., 2005, 2006a; Kraiczy et al., 2009) and can serve as a good internal control of protein mobility.

2.4. Site-directed mutagenesis

To insert an additional Met residue into BBA69 to obtain additional Se-Met residues for a sufficient anomalous signal during diffraction data collection, residue Leu214 was replaced by Met using a site-directed mutagenesis approach. Two complimentary primers were used (Table 1) for PCR amplification of the pETm-11-$BBA69_{76–263}$ construct followed by *DpnI* endonuclease digestion and transformation in *E. coli* XL1-Blue cells as described above. The presence of the Leu214Met mutation was confirmed by DNA sequencing (Fig. S2).

2.5. Crystallization of native and truncated protein

Initial crystallization screens for BBA69 in 96-well sitting-drop vapor diffusion plates were performed by a Tecan Freedom EVO 100 crystallization robot (Tecan Group Ltd.) by using the Structure Screen 1 &2 and JCSG + screens from Molecular Dimensions. The first crystal hits were obtained in a precipitant solution containing 0.2 M sodium acetate, 0.1 M Tris HCl (pH 8.5) and 30% PEG 4000, and after optimization, the crystals used for data collection were grown in 0.1 M ammonium sulfate, 0.1 M Tris HCl (pH 8.0) and 25% PEG 3350. To grow Se-Met-derived crystals, the same procedure and conditions were applied. During crystal harvesting, the concentration of PEG 3350 in the precipitant solution was increased to 38%, and PEG 3350 was used

Table 1
Oligonucleotides used in the study.

Oligonucleotide	Sequence (5'-3')	Application
BBA69 Forw.1	CAT GCC ATG GGC GCA AAT GAA AAC ACC AAG	Used for amplification of $BBA69_{35–263}$
BBA69 Forw.2	CAT GCC ATG GGC GGA ACT ACC GCT TCA GAG	Used for amplification of $BBA69_{76–263}$
BBA69 Rev.	GCT TGC GGC CGC TTA ATA AAA GGC AGA TTG TAA AGA	Used for amplification of BBA69
CspA Forw.	CAT GCC ATG GGC GAT GAA AAA ATT ATG GAA	Used for amplification of $CspA_{65–251}$
CspA Rev.	GCT TGC GGC CGC TTA GTA AAA GGC AGG TTT TAA	Used for amplification of $CspA_{65–251}$
BBA69 L-M1	CAA GTA AAA TCT GCC ATG CAG CTA CAA GAA AAG	Used for site-directed mutagenesis Leu214Met
BBA69 L-M2	CTT TTC TTG TAG CTG CAT GGC AGA TTT TAC TTG	Used for site-directed mutagenesis Leu214Met

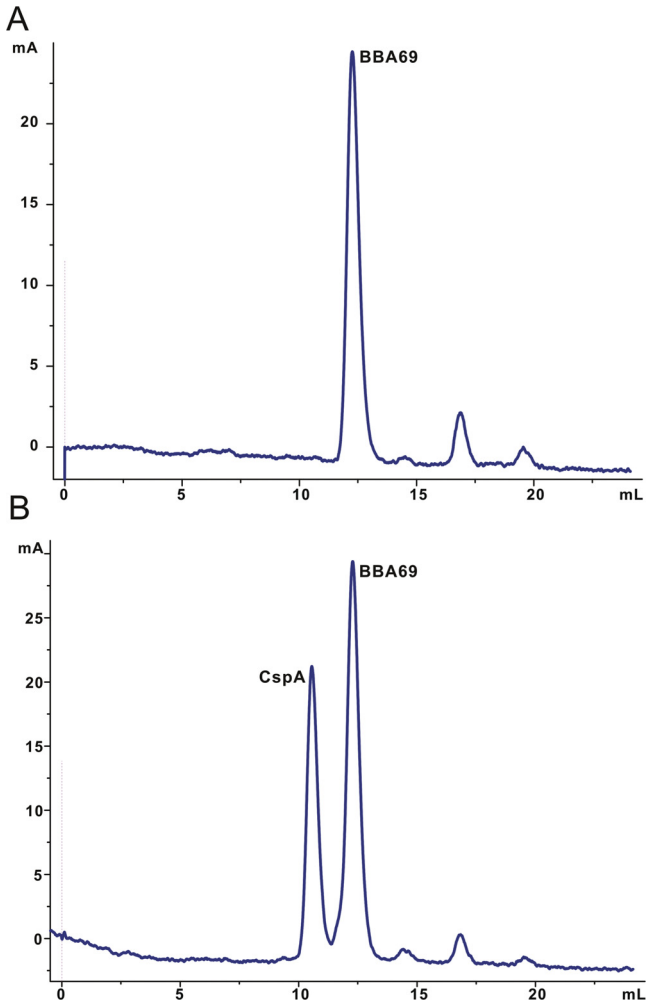

Fig. 1. Monomeric state of BBA69 as confirmed by size-exclusion chromatography. (A) BBA69 protein loaded on a prepacked Superdex 75 10/300 GL column; (B) mixture of CspA and BBA69 loaded on gel filtration column.

as a cryoprotectant when the crystals were flash-frozen in liquid nitrogen.

2.6. Data collection and structure determination

Native diffraction data were collected at MAX-lab beamline I911-3 (Lund, Sweden). X-ray diffraction data were subsequently collected from Se-Met-derived protein crystals at MX beamline instrument BL14.1 at the Helmholtz-Zentrum Berlin (Mueller et al., 2012). The crystal structure of BBA69 was determined by using the SAD method. The diffraction data were processed by MOSFLM and XDS and scaled by SCALA and AIMLESS from the CCP4 suite (Evans, 2011; Kabsch, 2010; Winn et al., 2011). Phase for Se-Met-derived protein were obtained using SHELX C/D/E (Sheldrick, 2008). The protein model was built automatically in Buccaneer (Cowtan, 2006), and manual improvement of the model was performed in Coot (Emsley and Cowtan, 2004). Crystallographic refinement was performed with REFMAC5 (Murshudov et al., 1997) (Fig. S3). A summary of the data collection, refinement and validation statistics is presented in Table 2.

3. Results and discussion

3.1. Protein production and structure determination

Because BBA69 is an outer surface lipoprotein with an N-terminal signal sequence, as predicted by SignalP 4.1 and LipoP 1.0 (Juncker et al., 2003; Petersen et al., 2011) and also observed in the other PFam54 members (Brangulis et al., 2013a, 2014; Brangulis et al., 2013b; Cordes et al., 2005), the initial recombinant protein produced excluded the signal peptide and contained residues 35-263. Unfortunately, the protein did not produce any diffraction-quality crystals even after extensive screening. Therefore, another construct containing a further shortened protein including residues 76–263 was produced; this applied the same strategy used for the production of PFam54 members BBA66 and BGA71 (Brangulis et al., 2014, 2018). The decision to shorten the recombinant protein was also based on sequence comparison with the PFam54 member CspA, the crystal structure of which has already been solved (Fig. 2). CspA was preferred for sequence comparison with BBA69, as the two sequences exhibit 61% sequence identity, in contrast to the only 17–20% identity between BBA69 and the paralogous proteins BBA64, BBA66 and BBA73. Additionally, recombinant CspA, including residues 26–250, was produced for crystallization, but in the crystal structure, only residues 70–250 were modeled due to the flexible nature of the N-terminus (Cordes et al., 2005). A comparison of both sequences clearly indicated that the structural domain of BBA69 should begin near residue 76. The shortened BBA69 construct comprising residues 76–263 was crystallized and diffraction data were collected; unfortunately, we failed to solve the structure by molecular replacement with the paralogous protein CspA as a model despite their 61% sequence identity. Furthermore, we also failed to solve the structure by using data from the Se-Met-derived protein, as only two Met residues (including the Met from the expression tag) were present in the protein. By applying site-directed mutagenesis, another Met residue was introduced, the protein was produced and crystallized, and diffraction data were collected accordingly. The crystal structure was solved in space group $P2_1$ and contained 4 molecules per asymmetric unit. The protein is composed of seven α-helices in a BbCRASP-1 fold, as observed in the crystal structures of the other PFam54 member proteins BBA64, BBA66, CspA and BBA73 (Brangulis

Table 2
Statistics for Data and Structure Quality.

Dataset	Native	Se-Met
Space group	P 2_1	C2
Unit cell dimensions		
a (Å)	67.26	73.97
b (Å)	96.09	110.55
c (Å)	67.35	61.70
Wavelength (Å)	1.0000	0.9797
Resolution (Å)	48.04-2.25	52.19-2.90
Highest resolution bin (Å)	2.32-2.25	3.08-2.90
No. of reflections	150291	40924
No. of unique reflections	39086	8521
Completeness (%)	99.8 (100.0)	96.7 (95.9)
$\mathbf{R_{merge}}$	0.04 (0.20)	0.06 (0.22)
$\boldsymbol{I/\sigma\ (I)}$	15.5 (5.1)	13.2 (5.6)
Multiplicity	3.8 (3.8)	4.8 (4.6)
Refinement		
$\mathbf{R_{work}}$	0.172 (0.187)	0.198 (0.199)
$\mathbf{R_{free}}$	0.248 (0.291)	0.267 (0.381)
Average B-factor (Å^2)		
Overall	36.2	69.0
From Wilson plot	22.5	62.4
No. of atoms		
Protein	6140	2999
Water	65	0
RMS deviations from ideal		
Bond lengths (Å)	0.011	0.006
Bond angles (°)	1.772	1.503
Ramachandran outliers (%)		
Residues in most favored regions (%)	97.28	95.49
Residues in allowed regions (%)	2.72	4.51
Outliers (%)	0.00	0.00

*Values in parentheses are for the highest resolution bin.

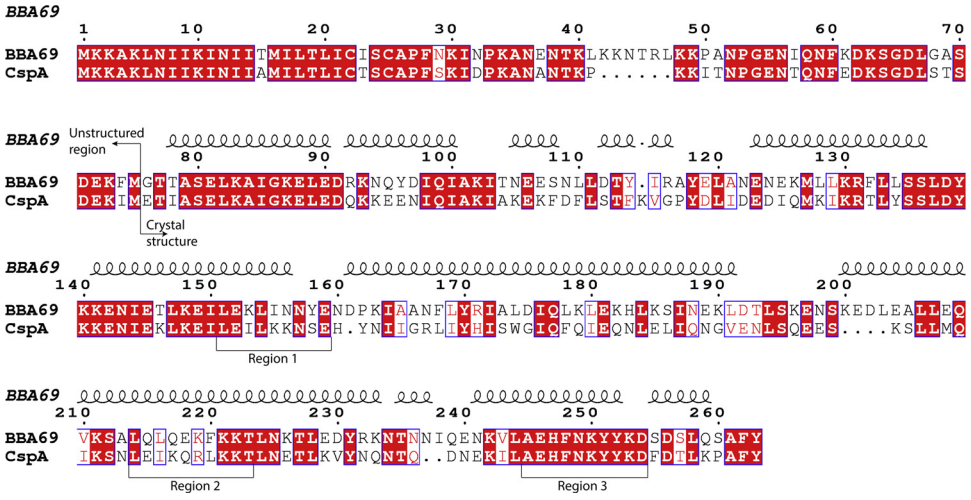

Fig. 2. Sequence alignment of the PFam54 members BBA69 and CspA. Initially, the alignment was performed by *Clustal Omega*, followed by processing of the sequence data with ESPript 3 (Robert and Gouet, 2014; Sievers et al., 2011). The conserved residues are written in white with a red background, while conserved substitutions are written in red and framed in blue. The secondary structure elements in BBA69 are illustrated above the alignment, while those in CspA are shown below the alignment. Residue numbering is shown for BBA69. Three regions in CspA thought to be involved in the binding of CFH and CFHL-1 are indicated (Kraiczy et al., 2004b, 2009) (For interpretation of the references to colour in this figure legend, the reader is referred to the web version of this article.).

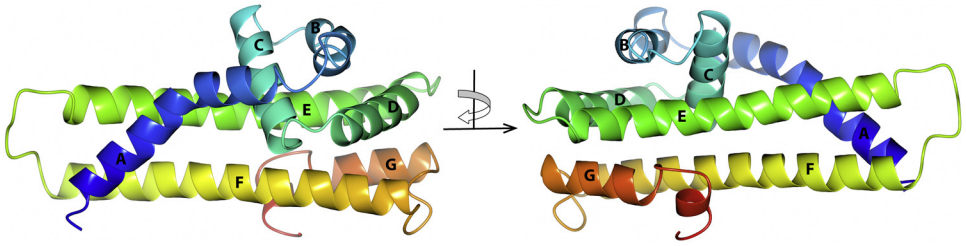

Fig. 3. The overall structure of *B. burgdorferi* BBA69 rotated by 180°. The protein is colored in blue at the N-terminus and ends in red at the C-terminus. All seven α-helices are labeled from A to G (For interpretation of the references to colour in this figure legend, the reader is referred to the web version of this article.).

et al., 2013a, 2014; Brangulis et al., 2013b; Cordes et al., 2005) (Fig. 3). The presence of the BbCRASP-1 fold was also confirmed by DALI server analysis, which did not find any other similar folds besides the common PFam54 fold (Holm and Laakso, 2016).

3.2. BBA69 as a member of the PFam54

As indicated in several previous studies, the primary sequence identity between PFam54 proteins is rather low; the sequence identity among most of the members is only slightly above 20%, and mainly nonpolar residues are conserved between the members (Brangulis et al., 2013a, 2014; Brangulis et al., 2013b; Cordes et al., 2006b). The nonpolar character of the conserved residues and the tendency of nonpolar residues to be oriented towards the protein core suggest that they are needed to preserve the common fold. In contrast to their low primary sequence identity, comparison of the *B. burgdorferi* PFam54 member protein structures determined so far reveals that the overall fold of the PFam54 members is very well preserved (Fig. 4). The main differences between the PFam54 member crystal structures are found at the C-terminus, where three possible variations are observed. In CspA, the C-terminal α-helix forms an extended conformation, which is in contrast to the other structures, but for the other PFam54 members with a bent C-terminal α-helices, they are of different lengths. In BBA69, the C-terminal α-helix, which runs along the structural domain, is much shorter than that in the other structures and does not cover the entire length of the protein. Some differences can also be observed in the loop regions, especially in the loop that follows α-helix A. This loop region in the BBA69 and CspA structures is more ordered and shorter than that in the structures of other PFam54 members, who show great diversity in the length and location of this loop region. Overall, it is easy to imagine that the PFam54 members possess different functions as judged from the low sequence identity; there are almost no conserved surface residues in addition to differences in the loop regions and lengths of the α-helices.

3.3. BBA69 and CspA

However, it is more interesting to look at the structural variation between the PFam54 members BBA69 and CspA, as BBA69, despite its comparatively higher sequence identity to CspA among the PFam54 members, is still unable to bind CFH and CFHL-1, and the potential reasons for this have been examined in several previous studies, although they were done without BBA69 structural data (Kraiczy et al., 2006, 2009; Wywial et al., 2009). Although there is no crystal structure of CspA in complex with either CFH or CFHL-1, its binding pattern has been investigated by PepSpot analysis and mutagenesis (Fig. 2) (Kraiczy et al., 2004b, 2009). In addition to the specific residues important for binding to CFH or CFHL-1, homodimerization of CspA, in which a

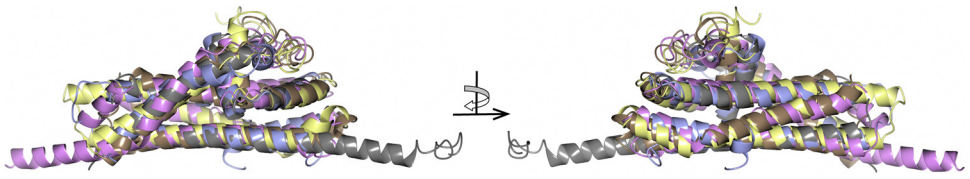

Fig. 4. Superimposed crystal structures of *B. burgdorferi* PFam54 members BBA69 (PDB ID 6QO1, blue), BBA64 (PDB ID 4ALY, brown), BBA66 (PDB ID 2YN7, yellow), BBA73 (PDB ID 4AXZ, pink) and CspA (PDB ID 1W33, gray). Structures are shown from two different angles and rotated by 180 degrees (For interpretation of the references to colour in this figure legend, the reader is referred to the web version of this article.).

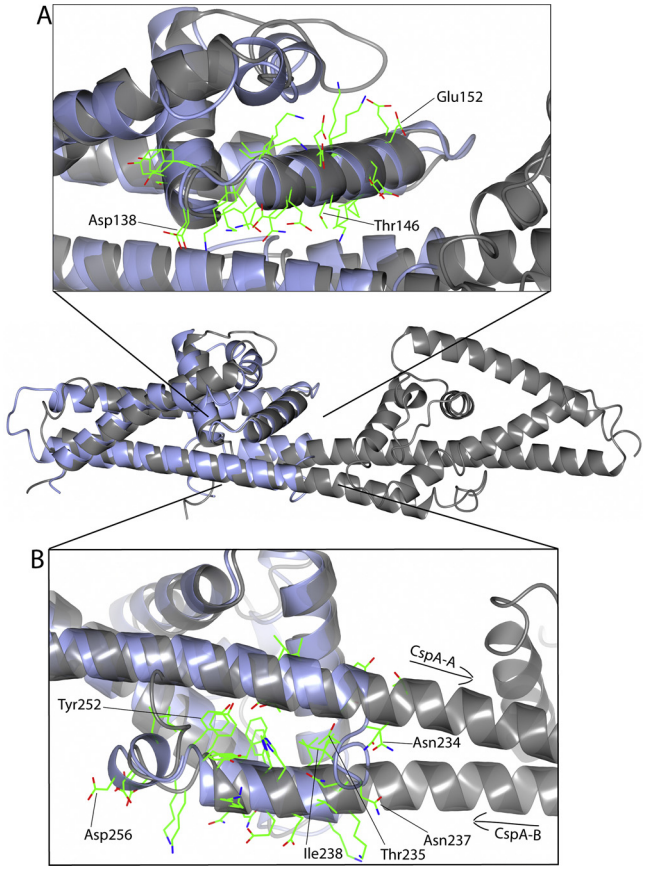

Fig. 5. Superimposed crystal structures of *B. burgdorferi* BBA69 (PDB ID 6QO1) and its paralogue CspA (PDB ID 1W33). (A) The residues in CspA involved in binding to CFH and CFHL-1 are indicated as bonds, and the corresponding residues in BBA69 are also shown. (B) Superimposed C-terminal α-helices of BBA69 and CspA, in which the conserved residues are shown as bonds. BBA69 is colored blue, while CspA is colored gray. Individual residues are specified in BBA69 (For interpretation of the references to colour in this figure legend, the reader is referred to the web version of this article.).

dimer interface between the C-terminal α-helices is created, is also essential for proper interaction (Cordes et al., 2006a; Kraiczy et al., 2009). By examining the residues important for binding to CFH and CFHL-1 in the crystal structure of CspA, and after superimposing the CspA structure with the crystal structure of BBA69, the differences that we assume account for the observed functional differences can be noticed immediately. First, the most obvious difference is the placement of the C-terminal α-helix, which is in an extended state in CspA, while it is bent and nestled along the protein in BBA69 (Fig. 5). In CspA, the C-terminal α-helix is necessary for dimerization and thus is important for the binding of CspA to CFH and CFHL-1 at the dimer interface (Kraiczy et al., 2006). According to the structural data, BBA69 is not able to form a homodimer in the same way as that observed for CspA, and, as confirmed by gel filtration chromatography, BBA69 is indeed a monomer and well separates from CspA dimer by size-exclusion chromatography (Fig. 1). These facts alone explain the differences in the abilities of both proteins to bind CFH and CFHL-1. In all previous studies, the C-terminal α-helix was assumed to have the same extended conformation as that observed in CspA and was modeled as such (Kraiczy et al., 2009; Wywial et al., 2009). In some respect, this was a rather logical conclusion, as both proteins show very high sequence identity at the C-terminal end (Fig. 2). The four C-terminal residues in BBA69 that are not conserved between the proteins (Ser255, Ser257, Gln259 and Ser260) were previously mutated to mimic the C-terminal α-helix in CspA; however, there no interaction with CFH/CFHL-1 was observed (Kraiczy et al., 2009). Although it was concluded that the C-terminal region is most likely not involved in CFH/CFHL-1 binding, to truly mimic the action of CspA would require adjusting the BBA69 segment, including residues 235-TNNIQEN-241, as that is the less conserved between the proteins and contains two additional residues (Asn237 and Ile238) in BBA69 that most likely are responsible for the conformational change in the C-terminal α-helix (Fig. 5b). In the superimposed crystal structures of BBA69 and the homodimer of CspA, it is striking that the C-terminal ends of both proteins overlay almost perfectly (Fig. 5b). Thus, the C-terminal residues Lys242-Tyr263 in BBA69 (α-helix G) are positioned in the same way as the end of the extended C-terminal α-helix in the other monomer of the CspA homodimer. Therefore, the same overall protein core seen in the other PFam54 members without the extended C-terminal α-helix has been maintained in CspA, but only on the condition that CspA forms a dimer, which thereby ensures that the missing C-terminal α-helix is in the same position as that in the other PFam54 members.

Second, the residues in CspA essential for binding to CFH/CFHL-1 are conserved, except the residue Lys141 in CspA, which is substituted by Thr146 in BBA69 (Fig. 5a). As shown previously, the CspA Lys141Thr mutant exhibited decreased binding with CFH/CFHL-1 compared to that observed with wild-type CspA; therefore, the corresponding mutation in the potential binding site does not explain the observed lack of CFH/CFHL-1 binding by BBA69 (Kraiczy et al., 2009).

Third, the electrostatic potential map clearly illustrates some surface charge differences between both proteins, including the proposed location of the CFH/CFHL-1 binding site, which further indicates the observed differences in the ability of the two proteins to bind CFH/CFHL-1 (Fig. 6).

4. Conclusions

It is likely that the PFam54 members evolved during gene duplication events, and CspA and BBA69 as the most closely related proteins among the PFam54 members, which has also been noted by previous studies (Wywial et al., 2009). As previously observed, the functions of

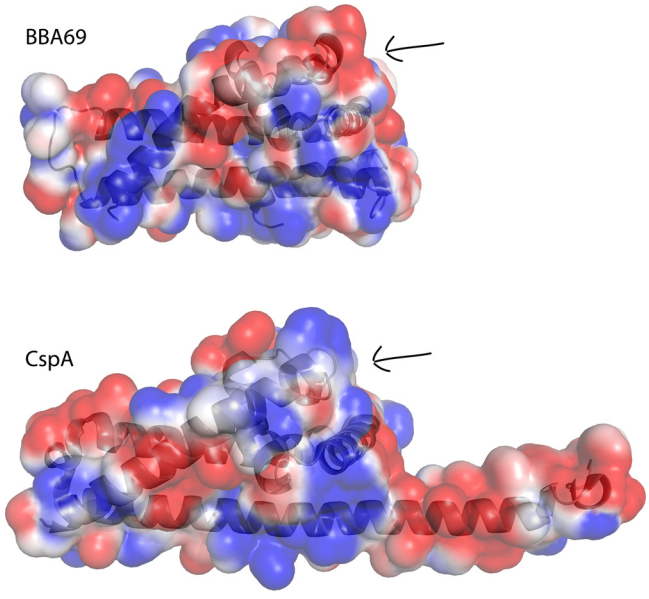

Fig. 6. Electrostatic surface potentials of *B. burgdorferi* BBA69 and its paralogue CspA. The electrostatic potentials (red, negative; blue, positive) were calculated using APBS (Jurrus et al., 2018), and the surface contour levels were set to −1 kT/e (red) and +1 kT/e (blue). The predicted binding site for CFH/CFHL-1 in CspA is indicated with an arrow in both proteins (For interpretation of the references to colour in this figure legend, the reader is referred to the web version of this article.).

both proteins differ, as BBA69 does not bind CFH/CFHL-1 (Kraiczy et al., 2006). Since the crystal structure of CspA has already been solved, the newly obtained crystal structure of BBA69 allowed us to make a structural comparison to reveal the molecular details responsible for this observed variation in function. In general, the comparison of both crystal structures clearly illustrated structural divergence, and the main variation, which likely accounts for the variation in function, was observed at the C-terminal α-helix. Furthermore, since dimer formation in CspA is required for binding to CFH/CFHL-1, and the C-terminal α-helix is responsible for dimerization, we assumed that this structural change determined the ability of CspA to bind CFH/CFHL-1.

Accession numbers

The coordinates and structure factors for native and Se-Met BBA69 have been deposited in the Protein Data Bank with the accession numbers 6QO1 and 6ROC.

*Values in parentheses are for the highest resolution bin.

Acknowledgement

This work was supported by the European Regional Development Fund (ERDF) grant Nr. 1.1.1.2/VIAA/1/16/144 “Structural and functional studies of Lyme disease agent Borrelia burgdorferi outer surface proteins to reveal the mechanisms of pathogenesis with the intention to create a new vaccine”.

The native diffraction data from *B. burgdorferi* BBA69 crystals were collected at MAX-lab beamline I911-3 (Lund, Sweden), and we acknowledge the staff at the MAX-lab synchrotron for their support during data collection. The diffraction data from Se-Met-derived BBA69 crystals were collected on BL14.1 at the BESSY II electron storage ring operated by Helmholtz-Zentrum Berlin. We particularly acknowledge the help and support of Thomas Hauss during the experiment.

Appendix A. Supplementary data

Supplementary material related to this article can be found, in the online version, at doi:https://doi.org/10.1016/j.ttbdis.2019.06.009.

References

Angel, T.E., Luft, B.J., Yang, X., Nicora, C.D., Camp 2nd, D.G., Jacobs, J.M., Smith, R.D., 2010. Proteome analysis of *Borrelia burgdorferi* response to environmental change. PLoS One 5, e13800.

Brangulis, K., Petrovskis, I., Kazaks, A., Baumanis, V., Tars, K., 2013a. Structural characterization of the *Borrelia burgdorferi* outer surface protein BBA73 implicates dimerization as a functional mechanism. Biochem. Biophys. Res. Commun. 434, 848–853.

Brangulis, K., Petrovskis, I., Kazaks, A., Tars, K., Ranka, R., 2014. Crystal structure of the infectious phenotype-associated outer surface protein BBA66 from the Lyme disease agent *Borrelia burgdorferi*. Ticks Tick. Dis. 5, 63–68.

Brangulis, K., Tars, K., Petrovskis, I., Kazaks, A., Ranka, R., Baumanis, V., 2013b. Structure of an outer surface lipoprotein BBA64 from the Lyme disease agent *Borrelia burgdorferi* which is critical to ensure infection after a tick bite. Acta Crystallogr. D Biol. Crystallogr. 69, 1099–1107.

Brangulis, K., Jaudzems, K., Petrovskis, I., Akopjana, I., Kazaks, A., Tars, K., 2015. Structural and functional analysis of BB0689 from *Borrelia burgdorferi*, a member of the bacterial CAP superfamily. J. Struct. Biol. 192, 320–330.

Brangulis, K., Akopjana, I., Petrovskis, I., Kazaks, A., Kraiczy, P., Tars, K., 2018. Crystal structure of the membrane attack complex assembly inhibitor BGA71 from the Lyme disease agent *Borrelia bavariensis*. Sci. Rep. 8, 11286.

Brooks, C.S., Hefty, P.S., Jolliff, S.E., Akins, D.R., 2003. Global analysis of *Borrelia burgdorferi* genes regulated by mammalian host-specific signals. Infect. Immun. 71, 3371–3383.

Burgdorfer, W., Barbour, A.G., Hayes, S.F., Benach, J.L., Grunwaldt, E., Davis, J.P., 1982. Lyme disease-a tick-borne spirochetosis? Science 216, 1317–1319.

Casjens, S., Palmer, N., van Vugt, R., Huang, W.M., Stevenson, B., Rosa, P., Lathigra, R., Sutton, G., Peterson, J., Dodson, R.J., Haft, D., Hickey, E., Gwinn, M., White, O., Fraser, C.M., 2000. A bacterial genome in flux: the twelve linear and nine circular extrachromosomal DNAs in an infectious isolate of the Lyme disease spirochete *Borrelia burgdorferi*. Mol. Microbiol. 35, 490–516.

Cordes, F.S., Roversi, P., Kraiczy, P., Simon, M.M., Brade, V., Jahraus, O., Wallis, R., Skerka, C., Zipfel, P.F., Wallich, R., Lea, S.M., 2005. A novel fold for the factor H-binding protein BbCRASP-1 of *Borrelia burgdorferi*. Nat. Struct. Mol. Biol. 12, 276–277.

Cordes, F.S., Kraiczy, P., Roversi, P., Simon, M.M., Brade, V., Jahraus, O., Wallis, R., Goodstadt, L., Ponting, C.P., Skerka, C., Zipfel, P.F., Wallich, R., Lea, S.M., 2006a. Structure-function mapping of BbCRASP-1, the key complement factor H and FHL-1 binding protein of *Borrelia burgdorferi*. Int. J. Med. Microbiol. 296 (Suppl 40), 177–184.

Cordes, F.S., Kraiczy, P., Roversi, P., Simon, M.M., Brade, V., Jahraus, O., Wallis, R., Goodstadt, L., Ponting, C.P., Skerka, C., Zipfel, P.F., Wallich, R., Lea, S.M., 2006b. Structure-function mapping of BbCRASP-1, the key complement factor H and FHL-1 binding protein of *Borrelia burgdorferi*. Int. J. Med. Microbiol. 296 (Suppl 40), 177–184.

Cowtan, K., 2006. The Buccaneer software for automated model building. 1. Tracing protein chains. Acta Crystallogr. D Biol. Crystallogr. 62, 1002–1011.

Emsley, P., Cowtan, K., 2004. Coot: model-building tools for molecular graphics. Acta Crystallogr. D Biol. Crystallogr. 60, 2126–2132.

Evans, P.R., 2011. An introduction to data reduction: space-group determination, scaling and intensity statistics. Acta Crystallogr. D Biol. Crystallogr. 67, 282–292.

Gilmore Jr., R.D., Howison, R.R., Schmit, V.L., Carroll, J.A., 2008. *Borrelia burgdorferi* expression of the bba64, bba65, bba66, and bba73 genes in tissues during persistent infection in mice. Microb. Pathog. 45, 355–360.

Gilmore Jr., R.D., Howison, R.R., Dietrich, G., Patton, T.G., Clifton, D.R., Carroll, J.A., 2010. The bba64 gene of *Borrelia burgdorferi*, the Lyme disease agent, is critical for mammalian infection via tick bite transmission. Proc. Natl. Acad. Sci. U. S. A. 107, 7515–7520.

Hart, T., Nguyen, N.T.T., Nowak, N.A., Zhang, F., Linhardt, R.J., Diuk-Wasser, M., Ram, S., Kraiczy, P., Lin, Y.P., 2018. Polymorphic factor H-binding activity of CspA protects Lyme borreliae from the host complement in feeding ticks to facilitate tick-to-host transmission. PLoS Pathog. 14, e1007106.

Holm, L., Laakso, L.M., 2016. Dali server update. Nucleic Acids Res. 44, W351–355.

Juncker, A.S., Willenbrock, H., Von Heijne, G., Brunak, S., Nielsen, H., Krogh, A., 2003. Prediction of lipoprotein signal peptides in Gram-negative bacteria. Protein Sci. 12, 1652–1662.

Jurrus, E., Engel, D., Star, K., Monson, K., Brandi, J., Felberg, L.E., Brookes, D.H., Wilson, L., Chen, J., Liles, K., Chun, M., Li, P., Gohara, D.W., Dolinsky, T., Konecny, R., Koes, D.R., Nielsen, J.E., Head-Gordon, T., Geng, W., Krasny, R., Wei, G.W., Holst, M.J., McCammon, J.A., Baker, N.A., 2018. Improvements to the APBS biomolecular solvation software suite. Protein Sci. 27, 112–128.

Kabsch, W., 2010. Xds. Acta. Crystallogr. D Biol. Crystallogr. 66, 125–132.

Kraiczy, P., Stevenson, B., 2013. Complement regulator-acquiring surface proteins of *Borrelia burgdorferi*: structure, function and regulation of gene expression. Ticks Tick. Dis. 4, 26–34.

Kraiczy, P., Rossmann, E., Brade, V., Simon, M.M., Skerka, C., Zipfel, P.F., Wallich, R., 2006. Binding of human complement regulators FHL-1 and factor H to CRASP-1 orthologs of *Borrelia burgdorferi*. Wien. Klin. Wochenschr. 118, 669–676.

Kraiczy, P., Hellwage, J., Skerka, C., Becker, H., Kirschfink, M., Simon, M.M., Brade, V., Zipfel, P.F., Wallich, R., 2004a. Complement resistance of *Borrelia burgdorferi* correlates with the expression of BbCRASP-1, a novel linear plasmid-encoded surface protein that interacts with human factor H and FHL-1 and is unrelated to Erp proteins. J. Biol. Chem. 279, 2421–2429.

Kraiczy, P., Hartmann, K., Hellwage, J., Skerka, C., Kirschfink, M., Brade, V., Zipfel, P.F., Wallich, R., Stevenson, B., 2004b. Immunological characterization of the complement regulator factor H-binding CRASP and Erp proteins of *Borrelia burgdorferi*. Int. J. Med. Microbiol. 293 (Suppl 37), 152–157.

Kraiczy, P., Hanssen-Hubner, C., Kitiratschky, V., Brenner, C., Besier, S., Brade, V., Simon, M.M., Skerka, C., Roversi, P., Lea, S.M., Stevenson, B., Wallich, R., Zipfel, P.F., 2009. Mutational analyses of the BbCRASP-1 protein of *Borrelia burgdorferi* identify residues relevant for the architecture and binding of host complement regulators FHL-1 and factor H. Int. J. Med. Microbiol. 299, 255–268.

Margos, G., Wilske, B., Sing, A., Hizo-Teufel, C., Cao, W.C., Chu, C., Scholz, H., Straubinger, R.K., Fingerle, V., 2013. *Borrelia bavariensis* sp. Nov. Is widely distributed in Europe and Asia. Int. J. Syst. Evol. Microbiol. 63, 4284–4288.

Mueller, U., Darowski, N., Fuchs, M.R., Forster, R., Hellmig, M., Paithankar, K.S., Puhringer, S., Steffien, M., Zocher, G., Weiss, M.S., 2012. Facilities for macromolecular crystallography at the Helmholtz-Zentrum Berlin. J. Synchrotron Radiat. 19, 442–449.

Murshudov, G.N., Vagin, A.A., Dodson, E.J., 1997. Refinement of macromolecular structures by the maximum-likelihood method. Acta Crystallogr. D Biol. Crystallogr. 53, 240–255.

Ojaimi, C., Brooks, C., Casjens, S., Rosa, P., Elias, A., Barbour, A., Jasinskas, A., Benach, J., Katona, L., Radolf, J., Caimano, M., Skare, J., Swingle, K., Akins, D., Schwartz, I., 2003. Profiling of temperature-induced changes in *Borrelia burgdorferi* gene expression by using whole genome arrays. Infect. Immun. 71, 1689–1705.

Patton, T.G., Brandt, K.S., Nolder, C., Clifton, D.R., Carroll, J.A., Gilmore, R.D., 2013. *Borrelia burgdorferi* bba66 gene inactivation results in attenuated mouse infection by tick transmission. Infect. Immun. 81, 2488–2498.

Petersen, T.N., Brunak, S., von Heijne, G., Nielsen, H., 2011. SignalP 4.0: discriminating signal peptides from transmembrane regions. Nat. Methods 8, 785–786.

Radolf, J.D., Caimano, M.J., Stevenson, B., Hu, L.T., 2012. Of ticks, mice and men: understanding the dual-host lifestyle of Lyme disease spirochaetes. Nat. Rev. Microbiol. 10, 87–99.

Robert, X., Gouet, P., 2014. Deciphering key features in protein structures with the new ENDscript server. Nucleic Acids Res. 42, W320–324.

Rudenko, N., Golovchenko, M., Grubhoffer, L., Oliver Jr., J.H., 2011. Updates on *Borrelia burgdorferi* sensu lato complex with respect to public health. Ticks Tick. Dis. 2,

123–128.
Sheldrick, G.M., 2008. A short history of SHELX. Acta Crystallogr. A 64, 112–122.
Sievers, F., Wilm, A., Dineen, D., Gibson, T.J., Karplus, K., Li, W., Lopez, R., McWilliam, H., Remmert, M., Soding, J., Thompson, J.D., Higgins, D.G., 2011. Fast, scalable generation of high-quality protein multiple sequence alignments using Clustal Omega. Mol. Syst. Biol. 7, 539.
Steere, A.C., Coburn, J., Glickstein, L., 2004. The emergence of Lyme disease. J. Clin. Invest. 113, 1093–1101.
Steere, A.C., Strle, F., Wormser, G.P., Hu, L.T., Branda, J.A., Hovius, J.W., Li, X., Mead, P.S., 2016. Lyme borreliosis. Nat. Rev. Dis. Primers 2, 16090.
Tokarz, R., Anderton, J.M., Katona, L.I., Benach, J.L., 2004. Combined effects of blood and temperature shift on *Borrelia burgdorferi* gene expression as determined by whole genome DNA array. Infect. Immun. 72, 5419–5432.
Winn, M.D., Ballard, C.C., Cowtan, K.D., Dodson, E.J., Emsley, P., Evans, P.R., Keegan, R.M., Krissinel, E.B., Leslie, A.G., McCoy, A., McNicholas, S.J., Murshudov, G.N., Pannu, N.S., Potterton, E.A., Powell, H.R., Read, R.J., Vagin, A., Wilson, K.S., 2011. Overview of the CCP4 suite and current developments. Acta Crystallogr. D Biol. Crystallogr. 67, 235–242.
Wywial, E., Haven, J., Casjens, S.R., Hernandez, Y.A., Singh, S., Mongodin, E.F., Fraser-Liggett, C.M., Luft, B.J., Schutzer, S.E., Qiu, W.G., 2009. Fast, adaptive evolution at a bacterial host-resistance locus: the PFam54 gene array in Borrelia burgdorferi. Gene 445, 26–37.